

Effective theory for ultracold strongly interacting fermionic atoms in two dimensions

Fan Wu¹, Jianshen Hu¹, Lianyi He^{1,2}, Xia-Ji Liu³, and Hui Hu³

¹*Department of Physics and State Key Laboratory of Low-Dimensional Quantum Physics, Tsinghua University, Beijing 100084, China*

²*Collaborative Innovation Center of Quantum Matter, Beijing 100084, China and*

³*Centre for Quantum and Optical Science, Swinburne University of Technology, Melbourne, Victoria 3122, Australia*

(Dated: June 21, 2019)

We propose a minimal theoretical model for the description of a two-dimensional (2D) strongly interacting Fermi gas confined transversely in a tight harmonic potential, and present accurate predictions for its equation of state and breathing mode frequency. We show that the minimal model Hamiltonian needs at least two independent interaction parameters, the 2D scattering length and effective range of interactions, in order to quantitatively explain recent experimental measurements at nonzero filling factor N/N_{2D} , where N is the total number of atoms and N_{2D} is the threshold number to reach the 2D limit. We therefore resolve in a satisfactory way the puzzling experimental observations of reduced equations of state and reduced quantum anomaly in breathing mode frequency, due to small yet non-negligible N/N_{2D} . We argue that a conclusive demonstration of the much-anticipated quantum anomaly is possible at a filling factor of a few percent. Our establishment of the minimal model for 2D ultracold atoms could be crucial to understanding the fermionic Berezinskii-Kosterlitz-Thouless transition in the strongly correlated regime.

Two-dimensional (2D) quantum many-body systems are of great interest, due to the interplay of reduced dimensionality and strong correlation, which leads to enhanced quantum and thermal fluctuations [1] and a number of ensuing quantum phenomena such as Berezinskii-Kosterlitz-Thouless (BKT) physics [2, 3]. In this respect, the recently realized 2D Fermi gas of ultracold ⁶Li and ⁴⁰K atoms under a tight axial confinement provides a unique platform [4, 5], with unprecedented controllability particularly on interatomic interactions. To date, many interesting properties of ultracold 2D Fermi gases have been thoroughly experimentally explored [5], including the equation of state (EoS) at both zero temperature [6, 7] and finite temperature [8, 9], radio-frequency spectroscopy [10–12], pair momentum distribution [13], first-order correlation function and BKT transition [14], and quantum anomaly in breathing mode frequency [15–17]. These results may shed light on understanding other important strongly correlated 2D systems, such as high- T_c layered cuprate materials [18], ³He submonolayers [19], exciton-polariton condensates [20] and neutron stars [21].

The present theoretical model of ultracold 2D Fermi gases is simple [4, 5]. Under a tight harmonic confinement with trapping frequency ω_z along the axial z -axis and a weak confinement ω_\perp in the transverse direction, the kinematic 2D regime is reached when the number of atoms N is smaller than a threshold $N_{2D} \simeq (\omega_z/\omega_\perp)^2$, so all the atoms are forced into the ground state of the motion along z [5]. The interatomic interactions are then described by a *single* s -wave scattering length a_{2D} [6], which is related to a 3D scattering length a_{3D} via the quasi-2D scattering amplitude [22]. Various experimental data have been compared and benchmarked with different theoretical predictions of the simple 2D model [23–32]. For EoS, i.e., the chemical potential and pressure at essentially zero temperature, good agreements were

found [6, 9]. But, at the *quantitative* level the experimental data in the strong interacting regime somehow lie systematically below the accurate predictions from auxiliary-field quantum Monte Carlo (AFQMC) simulations [6, 9]. The discrepancy is not so serious and might be viewed as an indicator of small deviation from the 2D kinematics [5], in spite of the fact that the 2D condition $N \ll N_{2D}$ is well satisfied. However, a serious problem does arise when two experimental groups measured the breathing mode frequency in the deep 2D regime most recently [16, 17]. The observed frequency turned out to be much smaller than the well-established theoretical prediction in the strongly interacting regime [25, 26]. This discrepancy is at the *qualitative* level, suggesting that the simple 2D model with a single parameter a_{2D} may not be sufficient for the description of ultracold 2D Fermi gases [33].

The purpose of this Letter is to provide a minimal theory of ultracold 2D Fermi gases, with the inclusion of a *properly* defined effective range of interactions (see Fig. 1). The proposed model Hamiltonian is then solved at zero temperature by taking into account strong pair fluctuations at Gaussian level and beyond (Fig. 2), with the help of a correlation energy from AFQMC in the zero-range limit [30]. This enables us to predict accurate EoS (Fig. 3 and Fig. 4), as well as reliable breathing mode frequency (Fig. 5). The puzzling quantitative and qualitative discrepancies, observed in the previous comparisons between experiment and theory [5, 6, 9, 16, 17], are therefore naturally resolved in a satisfactory way. Our results emphasize the important role played by the effective range of interactions in 2D strongly interacting Fermi systems, which may also be found in cuprate superconductors [18] and neutron stars [21].

Effective range of interactions. We start by considering the collision of two fermions with mass M and unlike spin in a highly anisotropic harmonic trapping potential,

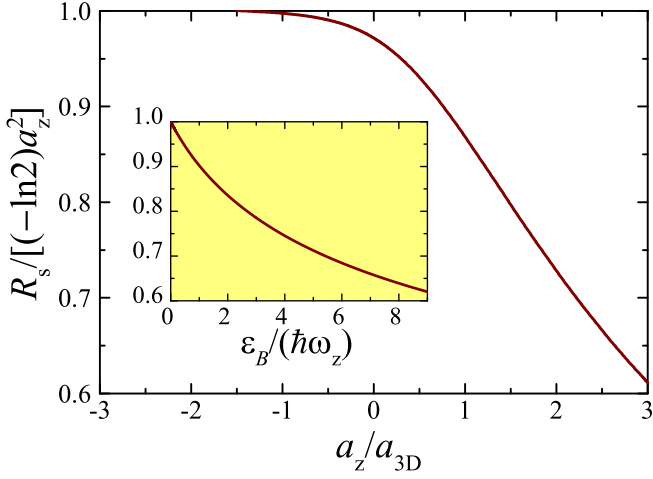


FIG. 1. Confinement-induced effective range of interactions R_s , in units of $R_s^{(0)} = (-\ln 2)a_z^2$, as a function of the inverse 3D scattering length a_z/a_{3D} . The inset shows the effective range as a function of the two-body binding energy.

described by a quasi-2D scattering amplitude [22],

$$f_{Q2D}(k; a_{3D}, a_z) = \frac{4\pi}{\sqrt{2\pi}a_z/a_{3D} + \varpi(k^2 a_z^2/2)}, \quad (1)$$

where $a_z \equiv \sqrt{\hbar/(M\omega_z)}$ is the harmonic oscillator length along the z -axis and the function $\varpi(x)$ has the expansion $\varpi(x \rightarrow 0) \simeq -\ln(2\pi x/\mathcal{B}) + (2\ln 2)x + i\pi$ with $\mathcal{B} \simeq 0.905$ [22]. In the simplest treatment, one may parameterize the quasi-2D collision using a 2D scattering length a_{2D} [5, 6], by setting the 2D scattering amplitude $f_{2D}(k; a_{2D}) = -2\pi/\ln[ka_{2D}(k)/i] = f_{Q2D}(k; a_{3D}, a_z)$. In general, one thus obtains a momentum-dependent $a_{2D}(k)$, which in the zero-energy limit takes the form $a_{2D}(k \rightarrow 0) = a_s \equiv a_z \sqrt{\pi/\mathcal{B}} \exp(-\sqrt{\pi/2}a_z/a_{3D})$ [22]. The advantage of this simple treatment is that the description *universally* depends on a single parameter a_{2D} , to be evaluated at a characteristic collision momentum k_0 , i.e., $k_0 = \sqrt{2M\tilde{\mu}}/\hbar$, where $\tilde{\mu}$ is the chemical potential that does not include the two-body binding energy [5, 6].

A more adequate parametrization of the 2D collision is to include an effective range of interactions R_s in the 2D scattering amplitude [35],

$$f_{2D}(k; a_s, R_s) = \frac{4\pi}{-2\ln(ka_s) - R_s k^2 + i\pi}, \quad (2)$$

whose pole gives a two-body bound state with binding energy $\varepsilon_B = \hbar^2 \kappa^2/M$, where the wavevector κ satisfies $R_s = 2\ln(\kappa a_s)/\kappa^2$. The same two-body bound state should be supported by the pole of the quasi-2D scattering amplitude in Eq. (1) as well. By setting $k \rightarrow i\kappa$ there, we find $\sqrt{2\pi}a_z/a_{3D} + \varpi[-\varepsilon_B/(2\hbar\omega_z)] = 0$ [36]. Therefore, we can directly calculate the effective range R_s , once ε_B or κ is solved at a given a_z/a_{3D} .

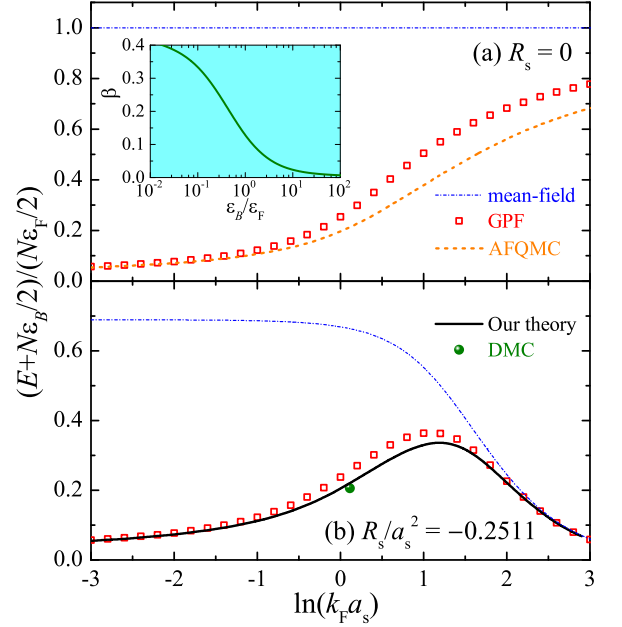


FIG. 2. Total energy with the two-body bound-state energy subtracted as a function of $\ln(k_F a_s)$, at $R_s = 0$ (a) and $R_s \simeq -0.2511a_s^2$ (b). The mean-field and GPF predictions are shown by blue dot-dashed lines and red squares, respectively. At zero range in (a), the latest AFQMC result [30] is plotted by orange dashed line. The inset shows the beta function $\beta(\varepsilon_B/\varepsilon_F)$. At finite range in (b), our theory (black solid line) is compared with the DMC data (green dot) [38].

The effective range obtained in this way is reported in Fig. 1. It decreases monotonically from $R_s^{(0)} \equiv (-\ln 2)a_z^2$ with increasing a_z/a_{3D} (main figure) or binding energy ε_B (inset). We note that $R_s^{(0)}$ can be easily derived from the second expansion term in $\varpi(x \rightarrow 0)$ and its magnitude, i.e., $R_s^{(0)} \sim a_z^2$, is a clear indication of the quasi-2D nature of atom collisions [5, 22]. As the wavefunction of two colliding atoms at distance within a_z is set by the full 3D contact interaction potential, these collisions can never be *purely* 2D. They can only be approximately treated as 2D, out of the range $\sim a_z$.

When should we care about the effective range R_s ? The answer depends on the characteristic collision momentum k_0 or the dimensionless effective range $k_0^2 R_s$. By taking the chemical potential of a non-interacting trapped Fermi gas, i.e., $\tilde{\mu} \simeq N\hbar\omega_\perp$ [5], we find $k_0^2 R_s \simeq -(2\ln 2)\sqrt{N/N_{2D}}$, which could be very significant, even though the 2D condition $N \ll N_{2D}$ is well satisfied.

Many-body theory. To account for the effective range R_s , it is convenient to adopt a two-channel model Hamiltonian (the area $\mathcal{S} = 1$) [33, 37, 38]:

$$\mathcal{H} = \sum_{\mathbf{k}\sigma=\{\uparrow,\downarrow\}} \xi_{\mathbf{k}} c_{\mathbf{k}\sigma}^\dagger c_{\mathbf{k}\sigma} + \sum_{\mathbf{q}} (2\xi_{\mathbf{q}/2} + \nu) b_{\mathbf{q}}^\dagger b_{\mathbf{q}} + g \sum_{kq} \left(b_{\mathbf{q}} c_{\mathbf{q}/2+\mathbf{k}\uparrow}^\dagger c_{\mathbf{q}/2-\mathbf{k}\downarrow}^\dagger + \text{h.c.} \right), \quad (3)$$

where $\xi_{\mathbf{p}} \equiv \hbar^2 \mathbf{p}^2 / (2M) - \mu$, and $c_{\mathbf{k}\sigma}$ and $b_{\mathbf{q}}$ are the annihilation operators of atoms and molecules in the open- and closed-channel, respectively. The channel coupling g is related to R_s , via $R_s = 4\pi^2 \hbar^4 / (M^2 g^2)$, and the detuning ν of molecules is tuned to reproduce the binding energy ε_B , i.e., $\nu = -\varepsilon_B + g^2 \sum_{\mathbf{k}} [\hbar^2 \mathbf{k}^2 / M + \varepsilon_B]^{-1}$ [33, 38]. It is useful to emphasize that, a finite effective range leads to non-negligible closed-channel population $\langle b_{\mathbf{q}}^\dagger b_{\mathbf{q}} \rangle \neq 0$. These are simply *virtual excitations* above the ground-state motion along the z -axis, necessarily created from quasi-2D collisions.

We solve the model Hamiltonian at different orders of approximation at zero temperature. Formally, the ground-state energy E may be decoupled as,

$$E[\ln(k_F a_s), k_F^2 R_s] = E_{\text{MF}} + \Delta E_{\text{GPF}} + \Delta E_c, \quad (4)$$

where $k_F = (2\pi n)^{1/2}$ is Fermi wavevector and $\varepsilon_F = \hbar^2 k_F^2 / (2M)$ is Fermi energy for a system with number density n . The mean-field (MF) theory provides the leading term E_{MF} , while the major correction arising from strong pair fluctuations at Gaussian level can be obtained by using the Gaussian pair fluctuation (GPF) theory [29, 33, 39–41], i.e., $\Delta E_{\text{GPF}} = E_{\text{GPF}} - E_{\text{MF}}$. The effect of pair fluctuations *beyond* Gaussian level may be characterized by a correlation energy ΔE_c , which is anticipated to be much smaller than ΔE_{GPF} . To see this, in Fig. 2(a) we plot the ground-state energy in the zero-range limit ($R_s = 0$), predicted by mean-field theory, GPF theory [29] and AFQMC simulation [30]. Indeed, the correlation energy given by the difference between the GPF and AFQMC energies is notably smaller than ΔE_{GPF} . In particular, ΔE_c becomes vanishingly small in the tight-binding limit of $\ln(k_F a_s) \rightarrow -\infty$ [29]. It is then useful to define a beta function $\beta = \Delta E_c / \Delta E_{\text{GPF}} \ll 1$, which varies as functions of the two dimensionless interaction parameters $\ln(k_F a_s)$ and $k_F^2 R_s$. For small $k_F^2 R_s$, however, it seems plausible to assume that β relies on a single parameter $\varepsilon_B / \varepsilon_F$, whose dependence can be readily extracted in the zero-range limit using the accurate AFQMC data, as shown in the inset of Fig. 2(a).

We thus establish a viable procedure to calculate the ground-state energy at nonzero effective range. For a given set $(k_F a_s, k_F^2 R_s)$, we first calculate the binding energy $\varepsilon_B / \varepsilon_F$ and determine the value of β . Both mean-field and GPF theories are then applied to obtain E_{MF} and ΔE_{GPF} , and consequently $\Delta E_c = \beta \Delta E_{\text{GPF}}$. In Fig. 2(b), we present $E = E_{\text{GPF}} + \Delta E_c$ in black line for a fixed ratio $R_s / a_s^2 \simeq -0.2511$, at which we may benchmark our prediction against available diffusion Monte Carlo (DMC) data (i.e., the single green dot) [38, 42]. We find that the correction ΔE_{GPF} becomes smaller at nonzero effective range. Towards the non-interacting limit ($a_s \rightarrow \infty$) and hence large $k_F^2 R_s$, ΔE_{GPF} vanishes quickly. This is understandable, since pair fluctuations become weaker with decreasing channel coupling g and even mean-field theory may provide accurate prediction

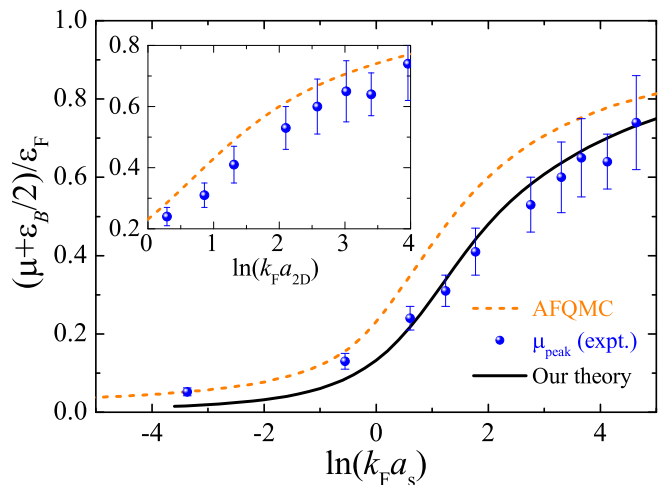


FIG. 3. Chemical potential with the two-body bound state contribution subtracted, as a function of $\ln(k_F a_s)$ at the number of atoms $N = N_{2D}$. The predictions of AFQMC (i.e., for zero effective range) [30] and our theory with a realistic effective range as in the experiment [9] are shown by orange dashed line and black solid line, respectively, and are compared with the experimental data for μ_{peak} (blue circles) measured at $N \simeq N_{2D}$ [9, 44]. The inset shows the chemical potential as a function of $\ln(k_F a_{2D})$, where a_{2D} is the effective scattering length adopted in the experiment [9].

at sufficiently large $k_F^2 R_s$ [38]. The correlation energy also significantly reduces at finite effective range and we find $|\Delta E_c| < 0.02 N \varepsilon_F$ at all interaction strengths. The agreement between our theory with DMC is excellent. The difference is less than $0.01 N \varepsilon_F$ and is comparable to the systematic error of standard QMC simulation [23].

Equation of state. Once the ground-state energy E of a uniform 2D Fermi gas is determined, we calculate directly the chemical potential μ and pressure P using standard thermodynamic relations. Experimentally, these *homogeneous* EoS can be extracted from a low-temperature trapped Fermi gas, by using the local density approximation [43], which assigns a local chemical potential $\mu(r) = \mu_{\text{peak}} - V(r)$ to each position r in the potential $V(r) = M\omega_{\perp}^2 r^2 / 2$. Both the peak chemical potential μ_{peak} and the *in situ* density distribution $n(r)$ can be experimentally measured [6, 8, 9], from which one deduces the homogeneous density EoS $n(\mu)$. By further using the force balance condition [6], $\nabla P(r) = -n(r)\nabla V(r)$, the homogeneous pressure EoS $P(n)$ can also be determined.

In Fig. 3, we show the experimental data for the peak chemical potential μ_{peak} , measured at different magnetic fields (i.e., a_{3D}) and hence at different $\ln(k_F a_s)$ [9, 44]. Our predictions for the peak chemical potential, calculated under the same experimental condition, are plotted by the black solid line. We find a good agreement between theory and experiment. Due to the large effective range of interactions in the experiment (i.e., $k_F^2 R_s \lesssim -1.2$ at $N \simeq N_{2D}$ [9]), the zero-range predic-

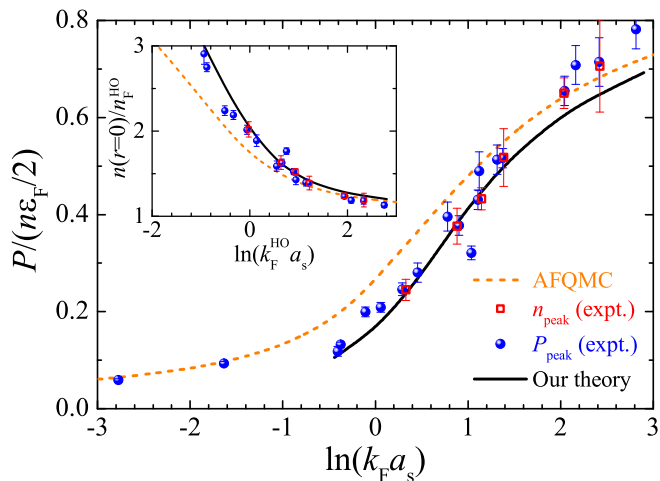


FIG. 4. Pressure as a function of $\ln(k_F a_s)$ at $N = 0.35N_{2D}$. We use blue circles and red squares to show the experimental data from Ref. [6] and Ref. [7] with $N \simeq 0.35N_{2D}$, respectively. The predictions of AFQMC [30] and our theory are shown by orange dashed line and black solid line, respectively. Towards the weakly interacting limit, the finite-temperature effect may become sizable and up-shift the pressure data [6]. The inset shows the peak density (in units of n_F^{HO}) as a function of $\ln(k_F^{\text{HO}} a_s)$, where n_F^{HO} and $k_F^{\text{HO}} = (2\pi n_F^{\text{HO}})^{1/2}$ are the peak density and wave-vector of an ideal Fermi gas in traps.

tions from AFQMC appear to strongly over-estimate the chemical potential. The use of an *effective* 2D scattering length a_{2D} can not fully explain the discrepancy (see the inset and also Fig. 1 in Ref. [9]), as we mentioned earlier.

In Fig. 4, we present the comparison between our predictions and the experimental data [6, 7] for pressure at the trap center. In this case, we have $N \simeq 0.35N_{2D}$ and therefore the effect of the effective range may become weaker. Nevertheless, we can see clearly that in the strongly interacting regime (i.e., $0 < \ln(k_F a_s) < 2$), the experimental data lie systematically below the zero-range results from AFQMC. The model Hamiltonian with a finite effective range should be used, in order to quantitatively understand the experimental measurement. We note that, in harmonic traps the pressure at the center is fixed by the force balance condition to $P = M\omega_\perp^2 N / (2\pi)$ [7]. Using the peak density of an ideal trapped Fermi gas $n_F^{\text{HO}} = M\omega_\perp \sqrt{N} / (\pi\hbar)$ [5], we find that the peak density $n \equiv n(r=0)$ can be written in terms of the pressure at the trap center, i.e., $n/n_F^{\text{HO}} = [P/(n\varepsilon_F/2)]^{-1/2}$. This provides an alternative way to illustrate the data, as shown in the inset. In the strongly interacting regime, the pronounced difference between the zero- and finite-range results is then better visualized.

Breathing mode and quantum anomaly. We now turn to consider the breathing mode frequency, which was recently measured in two experiments at $N \simeq 0.2N_{2D}$ [16, 17], as shown in Fig. 5 by green circles and blue squares. Theoretically, the zero-temperature breathing

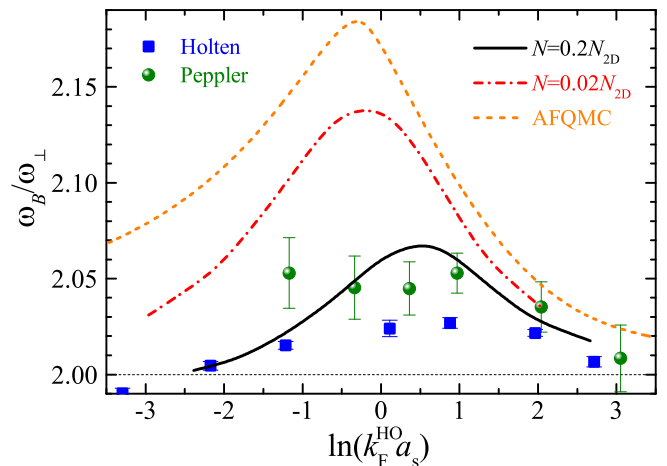


FIG. 5. Breathing mode frequency of 2D strongly interacting fermions as a function of the interaction parameter $\ln(k_F^{\text{HO}} a_s)$, at different total number of atoms $N/N_{2D} = 0$ (AFQMC [49], orange dashed line), 0.02 (red dot-dashed line) and 0.2 as in two recent experiments (black solid line). The experimental data at $N \simeq 0.2N_{2D}$ by Holten *et al.* [16] ($T = 0.10 - 0.18T_F$) and Peppler *et al.* [17] ($T = 0.14 - 0.22T_F$), where T_F is the Fermi temperature, are shown by green circles and blue squares, respectively.

mode frequency can be conveniently calculated by using the sum-rule approach [45, 46],

$$\hbar^2 \omega_B^2 = -2 \langle r^2 \rangle \left[\frac{d \langle r^2 \rangle}{d \langle \omega_\perp^2 \rangle} \right]^{-1}, \quad (5)$$

where $\langle r^2 \rangle = N^{-1} \int d^2r [r^2 n(r)]$ is the squared radius of the Fermi cloud at a given trapping frequency ω_\perp . In the classical treatment, a 2D Fermi gas is scale-invariant [47] and acquires a polytropic density EoS, $\mu(n) \propto n^2$. As a result, the mode frequency is pinned to $2\omega_\perp$, regardless of temperature and interactions [47]. The deviation of the breathing mode frequency away from $2\omega_\perp$ can be viewed a quantum anomaly [25, 26], arising from strong quantum pair fluctuations in 2D [48].

As readily seen from Fig. 5, the observed quantum anomaly in the two experiments is far below the prediction from AFQMC for zero-range interactions with a single 2D scattering length [49]. It can only be understood when we use the proposed minimal model for 2D ultracold fermions and take into account the realistic finite effective range at $N \simeq 0.2N_{2D}$. The quantitative difference between our theory and experiment at $0 < \ln(k_F a_s) < 1$ could be caused by the finite temperature in the two experiments, which is in the range $[0.10 - 0.22]T_F$.

It turns out that the breathing mode frequency or quantum anomaly depends sensitively on the effective range. The zero-range result of AFQMC can hardly be asymptotically approached, even we decrease the number of atoms down to just a few percent of N_{2D} (see the red dot-dashed line at $N = 0.02N_{2D}$). In this case, however,

the deviation from the classical limit of $2\omega_{\perp}$ is very significant and its experimental observation will constitute as a convincing proof of long-sought 2D quantum anomaly in cold atoms [48].

Conclusions. We have established a minimal model to describe ultracold interacting fermions confined in two dimensions and have solved it accurately. We have shown that the confinement-induced effective range of interactions has to be included, in order to understand the recent measurements on quantum anomaly in a qualitative manner and on equation of state at quantitative level. Our results pave the way to investigate the crucial role played by effective range in other two-dimensional quantum many-body systems and provide an excellent starting point to address the fermionic Berezinskii-Kosterlitz-Thouless transition with cold-atoms [14, 50].

We thank Igor Boettcher for useful discussions. This research was supported by the National Natural Science Foundation of China, Grant No. 11775123 (L.H.), National Key Research and Development Program of China, Grant No. 2018YFA0306503 (L.H.), and Australian Research Council's (ARC) Discovery Program, Grant No. FT140100003 (X.-J.L), Grant No. DP180102018 (X.-J.L), and Grant No. DP170104008 (H.H.).

-
- [1] M. Randeria, J.-M. Duan, and L.-Y. Shieh, Bound States, Cooper Pairing, and Bose Condensation in Two Dimensions, *Phys. Rev. Lett.* **62**, 981 (1989).
- [2] V. L. Berezinskii, Destruction of long-range order in one-dimensional and two-dimensional systems with a continuous symmetry group. II. Quantum systems, *Sov. Phys. JETP* **34**, 610 (1972) [*Zh. Eksp. Teor. Fiz.* **61**, 1144 (1971)].
- [3] J. M. Kosterlitz and D. J. Thouless, Ordering, metastability and phase transitions in two-dimensional systems, *J. Phys. C* **6**, 1181 (1973).
- [4] J. Levinsen and M. M. Parish, Strongly Interacting Two-Dimensional Fermi Gases, in *Annual Review of Cold Atoms and Molecules* (World Scientific, Singapore, 2015), Volume 3, Chapter 1, Pages 1-75.
- [5] A. V. Turlapov and M. Y. Kagan, Fermi-to-Bose crossover in a trapped quasi-2D gas of fermionic atoms, *J. Phys.: Condens. Matter* **29**, 383004 (2017).
- [6] V. Makhalov, K. Martiyanov, and A. Turlapov, Ground-State Pressure of Quasi-2D Fermi and Bose Gases, *Phys. Rev. Lett.* **112**, 045301 (2014).
- [7] K. Martiyanov, T. Barmashova, V. Makhalov, and A. Turlapov, Pressure profiles of nonuniform two-dimensional atomic Fermi gases, *Phys. Rev. A* **93**, 063622 (2016).
- [8] K. Fenech, P. Dyke, T. Peppler, M. G. Lingham, S. Hoinka, H. Hu, and C. J. Vale, Thermodynamics of an Attractive 2D Fermi Gas, *Phys. Rev. Lett.* **116**, 045302 (2016).
- [9] I. Boettcher, L. Bayha, D. Kedar, P. A. Murthy, M. Neidig, M. G. Ries, A. N. Wenz, G. Zürn, S. Jochim, and T. Enss, Equation of State of Ultracold Fermions in the 2D BEC-BCS Crossover Region, *Phys. Rev. Lett.* **116**, 045303 (2016).
- [10] B. Fröhlich, M. Feld, E. Vogt, M. Koschorreck, W. Zwerger, and M. Köhl, Radio-Frequency Spectroscopy of a Strongly Interacting Two-Dimensional Fermi Gas, *Phys. Rev. Lett.* **106**, 105301 (2011).
- [11] A. T. Sommer, L. W. Cheuk, M. J. H. Ku, W. S. Bakr, and M. W. Zwierlein, Evolution of Fermion Pairing from Three to Two Dimensions, *Phys. Rev. Lett.* **108**, 045302 (2012).
- [12] Y. Zhang, W. Ong, I. Arakelyan, and J. E. Thomas, Polaron-to-Polaron Transitions in the Radio-Frequency Spectrum of a Quasi-Two-Dimensional Fermi Gas, *Phys. Rev. Lett.* **108**, 235302 (2012).
- [13] M. G. Ries, A. N. Wenz, G. Zürn, L. Bayha, I. Boettcher, D. Kedar, P. A. Murthy, N. Neidig, T. Lompe, and S. Jochim, Observation of Pair Condensation in the Quasi-2D BEC-BCS Crossover, *Phys. Rev. Lett.* **114**, 230401 (2015).
- [14] P. A. Murthy, I. Boettcher, L. Bayha, M. Holzmann, D. Kedar, M. Neidig, M. G. Ries, A. N. Wenz, G. Zürn, and S. Jochim, Observation of the Berezinskii-Kosterlitz-Thouless Phase Transition in an Ultracold Fermi Gas, *Phys. Rev. Lett.* **115**, 010401 (2015).
- [15] E. Vogt, M. Feld, B. Fröhlich, D. Pertot, M. Koschorreck, and M. Köhl, Scale Invariance and Viscosity of a Two-Dimensional Fermi Gas, *Phys. Rev. Lett.* **108**, 070404 (2012).
- [16] M. Holten, L. Bayha, A. C. Klein, P. A. Murthy, P. M. Preiss, and S. Jochim, Anomalous Breaking of Scale Invariance in a Two-Dimensional Fermi Gas, *Phys. Rev. Lett.* **121**, 120401 (2018).
- [17] T. Peppler, P. Dyke, M. Zamorano, S. Hoinka, and C. J. Vale, Quantum Anomaly and 2D-3D Crossover in Strongly Interacting Fermi Gases, *Phys. Rev. Lett.* **121**, 120402 (2018).
- [18] V. M. Loktev, R. M. Quick, and S. G. Sharapov, Phase fluctuations and pseudogap phenomena, *Phys. Rep.* **349**, 1 (2001).
- [19] M. Ruggeri, S. Moroni, and M. Boninsegni, Quasi-2D Liquid ^3He , *Phys. Rev. Lett.* **111**, 045303 (2013).
- [20] H. Deng, H. Haug, and Y. Yamamoto, Exciton-polariton Bose-Einstein condensation, *Rev. Mod. Phys.* **82**, 1489 (2010).
- [21] J. A. Pons, D. Viganò, and N. Rea, A highly resistive layer within the crust of x-ray pulsars limits their spin periods, *Nat. Phys.* **9**, 431 (2013).
- [22] D. S. Petrov and G. V. Shlyapnikov, Interatomic collisions in a tightly confined Bose gas, *Phys. Rev. A* **64**, 012706 (2001).
- [23] G. Bertaina and S. Giorgini, BCS-BEC Crossover in a Two-Dimensional Fermi Gas, *Phys. Rev. Lett.* **106**, 110403 (2011).
- [24] A. A. Orel, P. Dyke, M. Delehay, C. J. Vale, and H. Hu, Density distribution of a trapped two-dimensional strongly interacting Fermi gas, *New J. Phys.* **13**, 113032 (2011).
- [25] J. Hofmann, Quantum Anomaly, Universal Relations, and Breathing Mode of a Two-Dimensional Fermi Gas, *Phys. Rev. Lett.* **108**, 185303 (2012).
- [26] E. Taylor and M. Randeria, Apparent Low-Energy Scale Invariance in Two-Dimensional Fermi Gases, *Phys. Rev. Lett.* **109**, 135301 (2012).
- [27] M. Bauer, M. M. Parish, and T. Enss, Universal Equation

- of State and Pseudogap in the Two-Dimensional Fermi Gas, *Phys. Rev. Lett.* **112**, 135302 (2014).
- [28] M. Barth and J. Hofmann, Pairing effects in the nondegenerate limit of the two-dimensional Fermi gas, *Phys. Rev. A* **89**, 013614 (2014).
- [29] L. He, H. Lü, G. Cao, H. Hu, and X.-J. Liu, Quantum fluctuations in the BCS-BEC crossover of two-dimensional Fermi gases, *Phys. Rev. A* **92**, 023620 (2015).
- [30] H. Shi, S. Chiesa, and S. Zhang, Ground-state properties of strongly interacting Fermi gases in two dimensions, *Phys. Rev. A* **92**, 033603 (2015).
- [31] B. C. Mulkerin, K. Fenech, P. Dyke, C. J. Vale, X.-J. Liu, and H. Hu, Comparison of strong-coupling theories for a two-dimensional Fermi gas, *Phys. Rev. A* **92**, 063636 (2015).
- [32] E. R. Anderson and J. E. Drut, Pressure, Compressibility, and Contact of the Two-Dimensional Attractive Fermi Gas, *Phys. Rev. Lett.* **115**, 115301 (2015).
- [33] H. Hu, B. C. Mulkerin, U. Toniolo, L. He, and X.-J. Liu, Reduced Quantum Anomaly in a Quasi-Two-Dimensional Fermi Superfluid: Significance of the Confinement-Induced Effective Range of Interactions, *Phys. Rev. Lett.* **122**, 070401 (2019).
- [34] The definition of a 2D scattering length (denoted by a_2) used by Turlapov group in Ref. [6] and Ref. [7] is slightly different, and is related to a_{2D} by, $a_{2D} = (e^{\gamma_E}/2)a_2$, where $\gamma_E \simeq 0.577$ is Euler's constant.
- [35] S. K. Adhikari, Quantum scattering in two dimensions, *Am. J. Phys.* **54**, 362 (1986).
- [36] This equation can be rewritten as, $a_z/a_{3D} = \mathcal{F}[\varepsilon_B/(\hbar\omega_z)]$, where the function $\mathcal{F}(x)$ is given by, $\mathcal{F}(x) = \int_0^\infty du (4\pi u^3)^{-1/2} [1 - e^{-xu} / \sqrt{(1 - e^{-2u})/(2u)}]$.
- [37] X.-J. Liu and H. Hu, Self-consistent theory of atomic Fermi gases with a Feshbach resonance at the superfluid transition, *Phys. Rev. A* **72**, 063613 (2005).
- [38] L. M. Schonenberg, P. C. Verpoort, and G. J. Conduit, Effective-range dependence of two-dimensional Fermi gases, *Phys. Rev. A* **96**, 023619 (2017).
- [39] H. Hu, X.-J. Liu, and P. D. Drummond, Equation of state of a superfluid Fermi gas in the BCS-BEC crossover, *Europhys. Lett.* **74**, 574 (2006).
- [40] H. Hu, P. D. Drummond, and X.-J. Liu, Universal thermodynamics of strongly interacting Fermi gases, *Nat. Phys.* **3**, 469 (2007).
- [41] R. B. Diener, R. Sensarma, and M. Randeria, Quantum fluctuations in the superfluid state of the BCS-BEC crossover, *Phys. Rev. A* **77**, 023626 (2008).
- [42] The DMC simulations in Ref. [38] were carried out as a function of $k_F^2 r_{\text{eff}}^2 = 4k_F^2 R_s/\pi$ in the strongly interacting regime, where the mean-field solution for chemical potential μ_{MF} is fixed to 0. By solving the mean-field equation, we find the following relation between the effective range and 2D scattering length: $1/(k_F a_s) = [(\sqrt{1 - 4k_F^2 R_s} - 1)/(-2k_F^2 R_s)]^{1/2}$. The green dot in Fig. 2(b) corresponds to the DMC data at $k_F^2 r_{\text{eff}}^2 = -0.4$, leading to $k_F^2 R_s \simeq -0.31416$ and $k_F a_s \simeq 1.1185$. This gives the ratio $R_s/a_s^2 \simeq -0.2511$.
- [43] D. A. Butts and D. S. Rokhsar, Trapped Fermi gases, *Phys. Rev. A* **55**, 4346 (1997).
- [44] We have used the peak chemical potential data $\tilde{\mu}_0 = \mu_{\text{peak}} + \varepsilon_B/2$ listed in Table III of Supplemental Material of Ref. [9]. To have a robust procedure of measurement, in the experiment the chemical potential with the two-body binding energy subtracted ($\tilde{\mu}$) was assumed to be proportional to the local Fermi energy, $\tilde{\mu} = \varepsilon_F/c$ [9]. A ratio $1/c$ was then obtained by fitting the linear relation at different densities and was supposed to provide the same information as μ_{peak} at the trap center. The ratio $1/c$ is slightly smaller than $\tilde{\mu}_0/\varepsilon_F$, and is plotted in Fig. 1 of Ref. [9].
- [45] C. Menotti and S. Stringari, Collective oscillations of a one-dimensional trapped Bose-Einstein gas, *Phys. Rev. A* **66**, 043610 (2002).
- [46] H. Hu, G. Xianlong, and X.-J. Liu, Collective modes of a one-dimensional trapped atomic Bose gas at finite temperatures, *Phys. Rev. A* **90**, 013622 (2014).
- [47] L. P. Pitaevskii and A. Rosch, Breathing modes and hidden symmetry of trapped atoms in two dimensions, *Phys. Rev. A* **55**, R853 (1997).
- [48] M. Olshanii, H. Perrin, and V. Lorent, Example of a Quantum Anomaly in the Physics of Ultracold Gases, *Phys. Rev. Lett.* **105**, 095302 (2010).
- [49] We have calculated the density profile by using the AFQMC EoS and have then used the sum-rule equation (5) to determine the breathing mode frequency within AFQMC. This calculation improves the previous estimation given in Ref. [25] and Ref. [26].
- [50] B. C. Mulkerin, L. He, P. Dyke, C. J. Vale, X.-J. Liu, and H. Hu, Superfluid density and critical velocity near the Berezinskii-Kosterlitz-Thouless transition in a two-dimensional strongly interacting Fermi gas, *Phys. Rev. A* **96**, 053608 (2017).